

## One-dimensional N<sub>2</sub> gas inside single-walled carbon nanotubes

Christian Kramberger<sup>1\*</sup>, Theerapol Thurakitserree<sup>1</sup>, Heeyuen Koh<sup>1</sup>, Yudai Izumi<sup>2</sup>,  
Toyohiko Kinoshita<sup>2</sup>, Takayuki Muro<sup>2</sup>, Erik Einarsson<sup>1</sup>, and Shigeo Maruyama<sup>1</sup>

<sup>1</sup>Department of Mechanical Engineering, The University of Tokyo, 7-3-1 Hongo, Bunkyo-ku, Tokyo, 113-8656, Japan

<sup>2</sup>Japan Synchrotron Radiation Research Institute, 1-1-1 Kouto, Sayo, Hyogo, 679-5198, Japan

### Abstract

The unexpected presence of a linear arrangement of co-axially oriented N<sub>2</sub> molecules inside aligned single-walled carbon nanotubes is revealed by high resolution near-edge x-ray absorption spectroscopy. The encapsulated N<sub>2</sub> molecules exhibit free stretching vibrations with a long electronic lifetime of the x-ray-excited anti-bonding  $\pi^*$  states. Molecular dynamics simulations confirm that narrow-diameter nanotubes ( $d < 1$  nm) are crucial for stabilizing the linear arrangement of aligned N<sub>2</sub> molecules.

### 1. Introduction

Single-walled carbon nanotubes (SWCNT) provide in their interior a protected, narrowly confined space for novel one-dimensional structures. Linear chains of fullerenes (peapods) and the inner walls of double-walled nanotubes made from such peapods, as well as the general class of encapsulated nanowires are only a few selected examples from this broad field of one-dimensional materials. [1–3] With regard to nitrogen filling, pioneering and contemporary work has typically utilized bamboo-structured multi-walled carbon nanotubes (MWCNT) or hollow carbon nitride (CN<sub>x</sub>) nanofibers. [4] Very interestingly, the host MWCNT are found to induce co-axial alignment of diatomic nitrogen molecules in the

---

\* E-mail address: [Christian.Krambergerer-Kaplan@univie.ac.at](mailto:Christian.Krambergerer-Kaplan@univie.ac.at) (C. Kramberger)

vicinity of their innermost walls. [5–7] For SWCNT, however, only very narrow SWCNT may ever be expected to provide sufficiently narrow, uniform confinement spaces suitable for a locked linear arrangement of individual N<sub>2</sub> molecules. Here we demonstrate that sub-nm thin SWCNT can indeed template a locked linear arrangement of N<sub>2</sub>. High resolution near-edge X-ray absorption (NEXAFS) and molecular dynamics (MD) simulations reveal the fingerprint and the dynamics of co-axially aligned N<sub>2</sub> in the interior of forests of vertically aligned SWCNT (VA-SWCNT).

## **2. Experimental**

Our VA-SWCNT are home-grown using no-flow chemical vapor deposition (CVD). [8–10] Briefly, bimetallic Co/Mo catalyst particles were obtained by dip-coating Si substrates into separate Mo-acetate and Co-acetate solutions containing 0.01 wt.% of the respective metal species. After reducing the dip-coated substrate under flowing Ar/H<sub>2</sub> (3% H<sub>2</sub>), the CVD chamber was evacuated and sealed. SWCNT were then synthesized at 800°C under the vapor pressure of 40μL of feedstock injected into the chamber. We refer to SWCNT synthesized using pure ethanol feedstock as EtSWCNT, and those synthesized from an ethanol mixture containing 5 vol.% acetonitrile (CH<sub>3</sub>CN) as 5%Ac-SWCNT.[11]

## **3. Results & Discussion**

Scanning electron microscopy (SEM) images of the 5 to 6 μm tall Et-SWCNT and 5%Ac-SWCNT forests are shown in Figure 1. They confirm the vertical alignment present in both batches of SWCNT material.

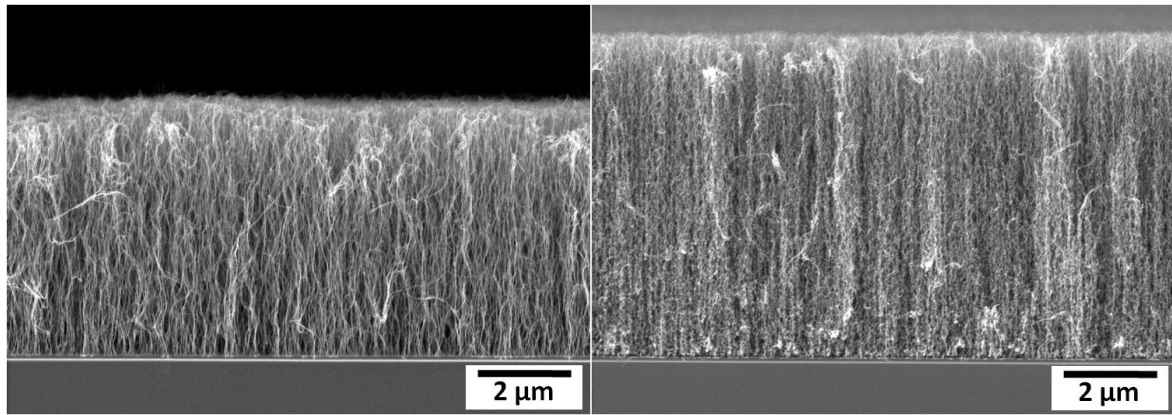


**Figure 1:** Side view SEM images of vertically aligned Et-SWCNT synthesized from pure ethanol (left panel) and 5%Ac-SWCNT synthesized from mixed feedstock containing 5 vol.% acetonitrile (right panel).

X-ray photoelectron spectroscopy (XPS) was performed using a PHI 5000 VersaProbe spectrometer. Figure 2 shows a narrow, asymmetric Doniach-Šunjić profile in the C1s of 5%Ac-SWCNT. The N1s of 5%Ac-SWCNT contains chemical shifts of molecular N<sub>2</sub> (near 404 eV) as well as the joint peak of incorporated N having pyridinic and substitutional configurations (398–400 eV). N1s peaks are never present in the XPS spectra of Et-SWCNT samples (not shown here). [11]

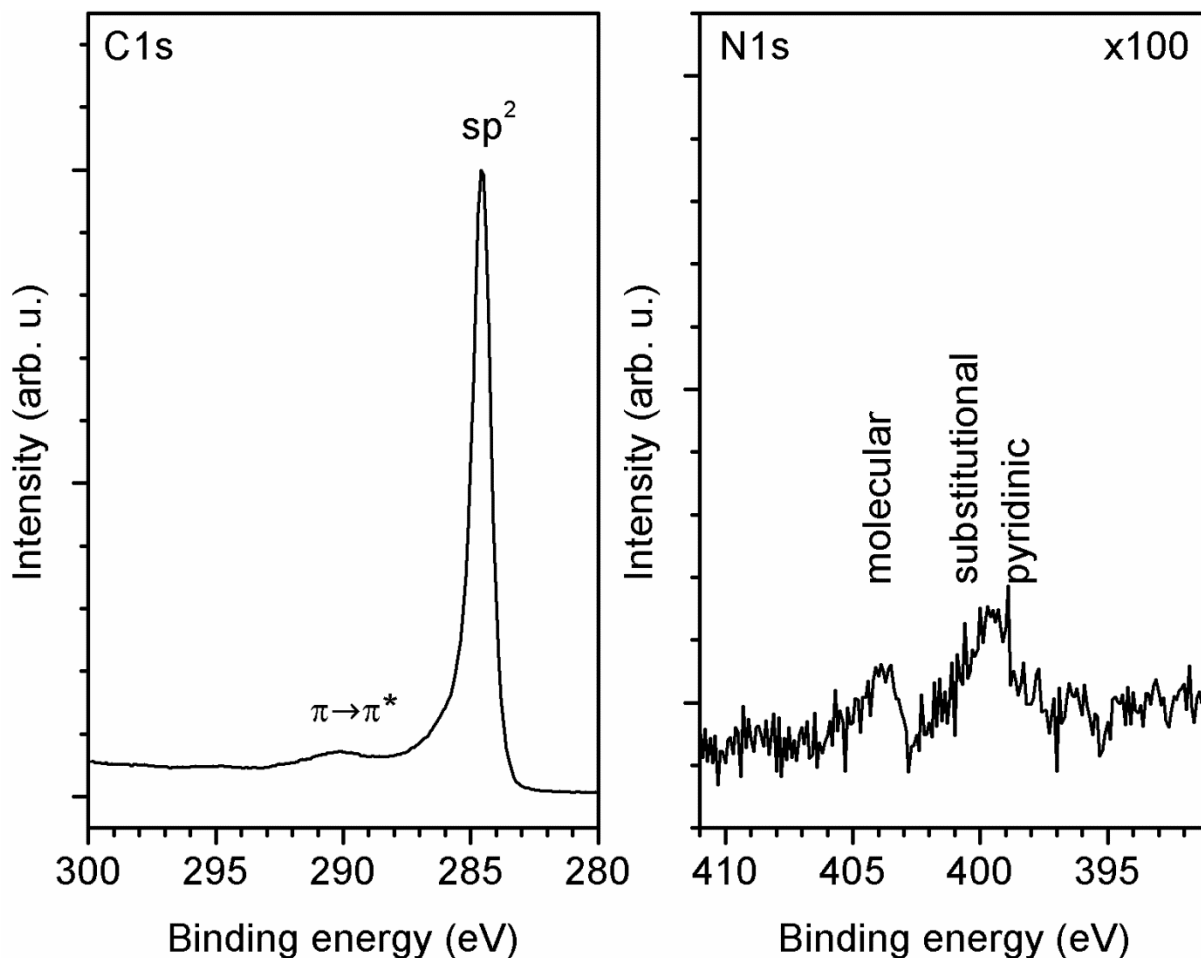


**Figure 2:** XPS spectra of C1s (left) and N1s (right) core electrons demonstrate the narrow, asymmetric Doniach-Šunjić resonance of the pure  $sp^2$  carbon network as well as molecular N<sub>2</sub> and incorporated nitrogen (both pyridinic and substitutional).

X-ray absorption spectroscopy (XAS) was conducted at BL27SU at the SPring-8 synchrotron facility. The beamline is dedicated to soft X-ray absorption spectroscopy. [12,13] All samples were baked at 400°C in ultra high vacuum ( $< 5 \times 10^{-9}$  mbar) in order to remove any atmospheric adsorbates before they were transferred to the experimental station. [14] The spectra were then recorded at ambient room temperature.

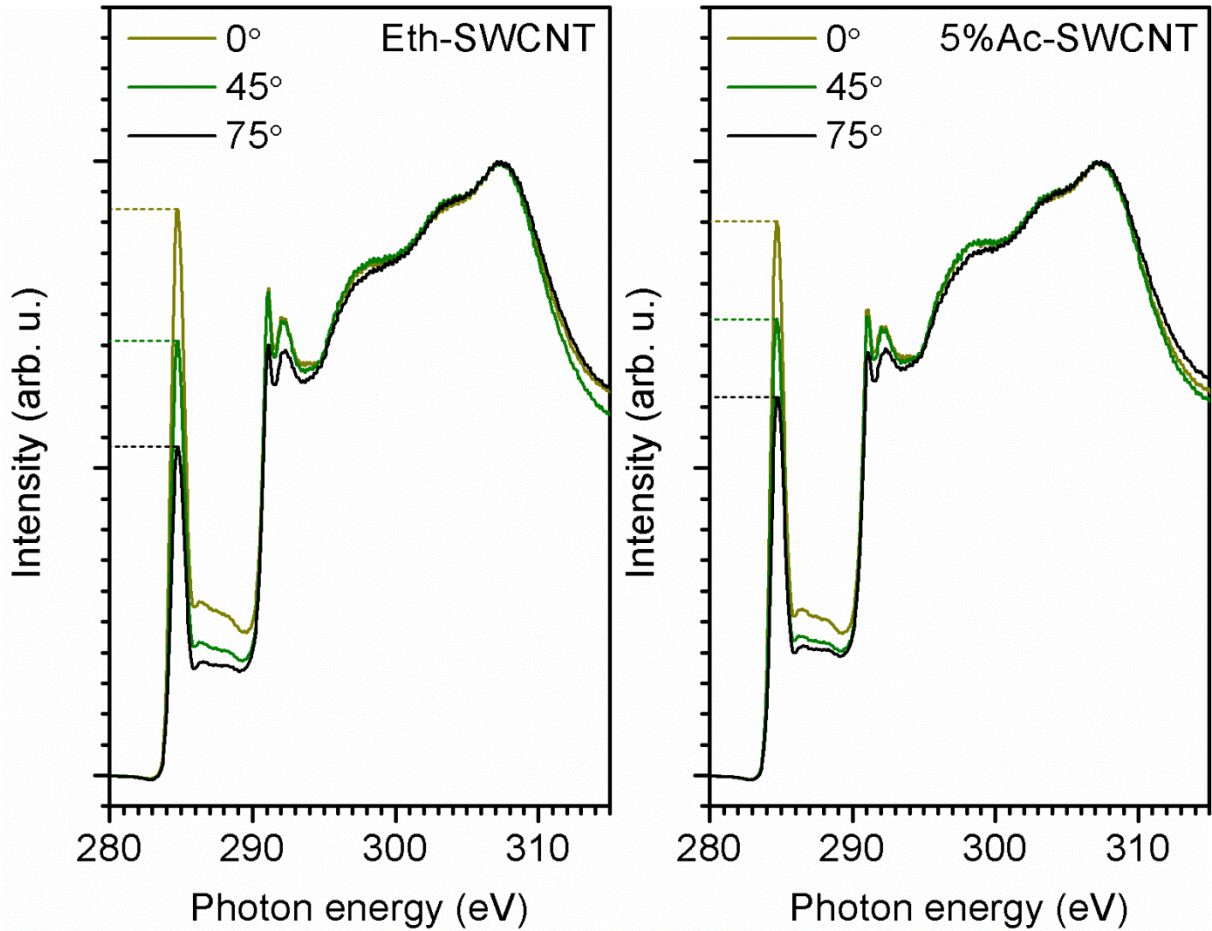


**Figure 3:** NEXAFS C1s spectra for different angles between the SWCNT alignment direction and the Poynting vector of the linearly polarized incident X-ray beam. Spectra are scaled to the maximum in the  $\sigma^*$  resonance.

The C1s edges of annealed Et-SWCNT and 5%Ac-SWCNT samples as seen in the XAS spectra in Figure 3 are virtually indistinguishable. The C1s $\rightarrow\pi^*$  resonance occurs at 284.6 eV and is followed by the transitions into  $\sigma^*$  states above 290 eV. The XAS spectra were recorded in drain current mode. Both batches of samples display in full detail the archetypical spectral shape of pure, high-quality SWCNT. [15] The nanotube alignment is probed by changing the angle between the linearly polarized X-ray beam and the vertical axis of the SWCNT forests. The mosaic spread of the  $\pi$  resonances are fitted with an offset cosine squared model function  $I_\pi(\phi) = A+B\cdot\cos^2(\phi)$ . The negative nematic order parameter  $\xi$  of the

co-planar orientation distribution of the  $C1s \rightarrow \pi^*$  transitions is directly accessed via Equation 1, in which  $I_{\parallel}$  and  $I_{\perp}$  refer to the orientation of the electric field vector with respect to the alignment direction of the nanotubes.

$$\xi = (I_{\parallel} - I_{\perp}) / (I_{\parallel} + 2I_{\perp}) \quad (1)$$

The nematic order parameter  $\xi$  of the aligned forests is the doubled positive of the negative nematic order parameter of  $C1s \rightarrow \pi^*$  transitions, and results in +0.25 for 5%Ac-SWCNT and +0.35 for Et-SWCNT. The somewhat lower nematic order compared with values obtained by optical absorption is related to the shallow probe depth of XAS ( $\sim 1$  nm at 300 eV) in comparison to actual bulk sensitivity of optical absorption that is measured in transmission.

[9]

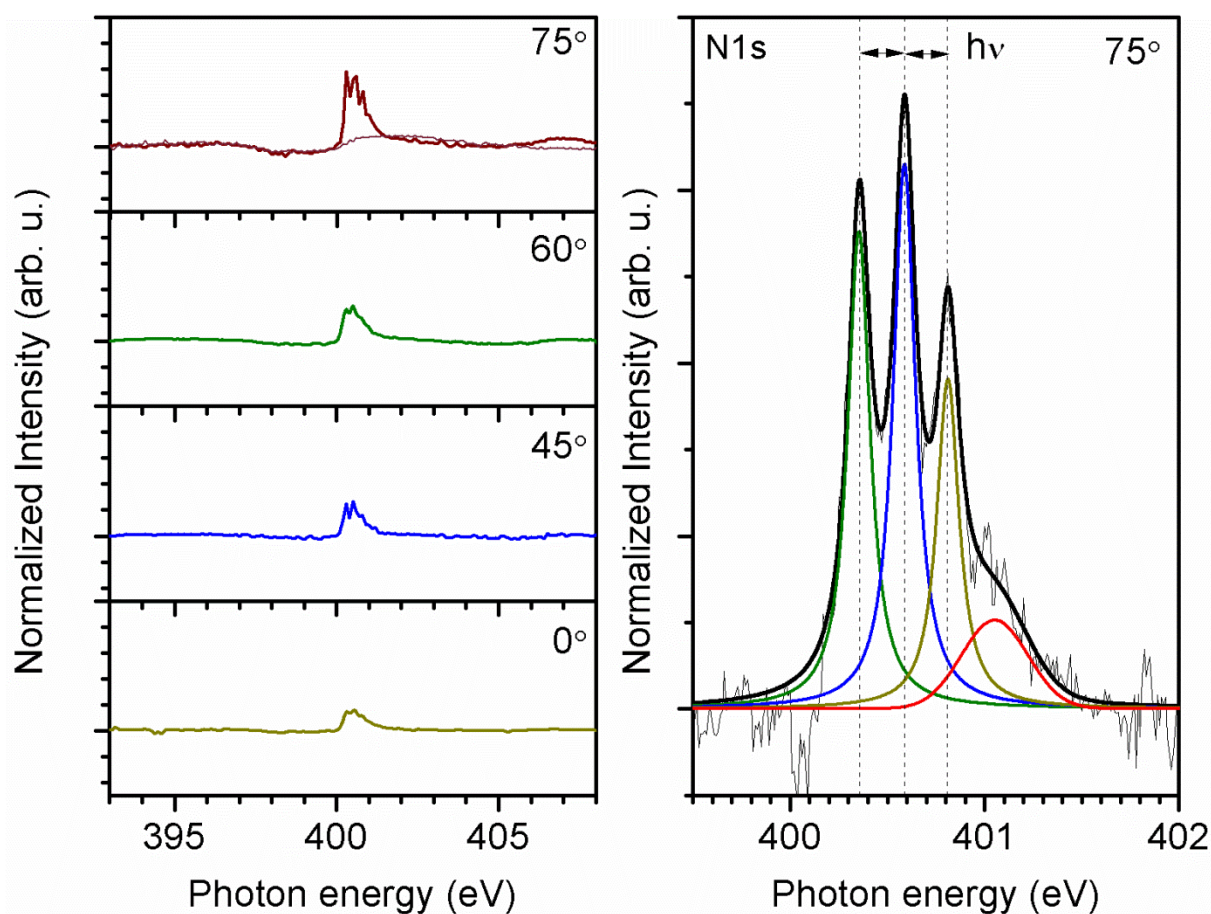


**Figure 4:** NEXAFS spectra of the N1s in VA-SWCNT grown from 5 vol.% acetonitrile/ethanol mixed feedstock. The left stack is for different angles between the incident X-ray beam and the SWCNT alignment axis. The thinner line in the topmost panel ( $75^\circ$ ) is the N1s-silent reference from SWCNT synthesized from pure ethanol feedstock. The right panel shows a high resolution scan of the vibrational fine structure in the N1s $\rightarrow\pi^*$  resonance and its lineshape analysis.

The N1s XAS spectra of the 5%Ac-SWCNT material is presented in Figure 4. The left panels show overview spectra of all possible N1s chemical shifts. Since the Et-SWCNT reference (thinner line in the  $75^\circ$  panel) is silent in the N1s, the presence of nitrogen in the 5%Ac-SWCNT is evidently related to the use of acetonitrile during synthesis. The first unexpected observation is that all N1s $\rightarrow\pi^*$  response comes from only one kind of chemical shift at 400.3 eV. The very weak and hardly noticeable signatures at 397 eV and 407 eV would match the expected positions of N1s $\rightarrow\pi^*$  and N1s $\rightarrow\sigma^*$  resonances of incorporated nitrogen. [5] XPS spectra in Figure 2 reveal comparable amounts of incorporated and molecular nitrogen. The very different observations are in part related to the different electronic escape depths at 400 eV and 1.483 keV, and mainly due to the different localization of the unoccupied electronic states in SWCNT walls and N<sub>2</sub> molecules. In XPS the unoccupied electronic states are not involved at all in the initial cross section and the subsequent electron escape process. [16] In contrast, XAS is apparently greatly enhanced on transitions into the lowest unoccupied molecular orbital in N<sub>2</sub> molecules. Furthermore, the dipole transitions from the N1s core level into unoccupied  $\pi^*$  states also probe the anisotropy of the local electronic structure and hence render XAS the ideally suited tool to investigate encapsulated N<sub>2</sub> inside small-diameter SWCNT.

The second observation that can be made is that the overall intensity of the spectra increases with the angle of incidence. For normal incidence ( $\phi = 0^\circ$ ) the X-ray electric field vector is perpendicular to the SWCNT alignment direction and the signal from the co-axially aligned  $N_2$  is depleted. In the limit of  $\phi \rightarrow 90^\circ$  the electric field vector becomes parallel to the aligned VA-SWCNT and the signal of the encapsulated  $N_2$  is strongly enhanced. The identification of  $N_2$  (400.3 eV) is further backed up by the opposite bond orientation than observed for cyanic N (399.5 eV), that would in the same geometry be enhanced for  $\phi = 0^\circ$ . [17] By taking into account the overall increase of signal, seen in the isotropic total edge jump of the C1s, the nematic order of the  $N_2$  molecules is  $\xi = 0.22$ . This is comparable to  $\xi = 0.25$  obtained from the C1s of the host 5%Ac-SWCNT. Since all samples were annealed at  $400^\circ\text{C}$  prior to measurement, and the N1s signal is not present in Et-SWCNT, the spectroscopic observations strongly suggest that the  $N_2$  molecules are inside the very narrow 5%Ac-SWCNT, and these molecules are furthermore co-axially aligned in the interior of sub-nm thin SWCNT.

The right panel of Figure 4 displays a high resolution scan of the  $N1s \rightarrow \pi^*$  resonance above 400.3 eV. The fine structures in the spectrum match in full detail the vibrational sidebands of the  $N_2$  molecule. We find a peak spacing of  $233 \pm 3$  meV, and the full width at half maxima of the individual Voigtian components are  $138 \pm 3$  meV. These values match the reference values for free  $N_2$  molecules well. [12,18] The effective c-axis of the confining space is infinite, which should—unlike a tight c-axis—have no effect on the line shape. [19,20] The unchanged lifetime of the X-ray-excited  $\pi$  states, as well as the unaltered vibrational levels, are in-line with one-dimensional containment.

In contrast to earlier reports on nitrogen-doped or  $N_2$ -filled MWCNT or  $CN_x$  nanofibers, we clearly have a one-dimensional  $N_2$  gas contained inside single-walled carbon nanotubes. [4-7,17] Since encapsulated  $N_2$  is not found for Et-SWCNT, the logical conclusion is that  $N_2$  enters the SWCNT during synthesis using acetonitrile. In this case, the C-N species

dissociates upon interaction with the catalyst particle. There is a small probability the dissolved N will be incorporated into the  $sp^2$  nanotube structure, but it is much more likely to encounter another N and form  $N_2$ . This stable  $N_2$  can then leave the catalyst, sometimes exiting into the interior of the growing SWCNT. This mechanism has been proposed for  $N_2$  filled  $CN_x$  nanofibers, and should also be applicable to the growth of SWCNT. [21]

For further insight into the behavior of  $N_2$  molecules inside very narrow SWCNT, we performed molecular dynamics (MD) simulations with four  $N_2$  molecules in the interior of 10 nm long (6,6) and (7,7) SWCNT. Corresponding diameters are 0.82 and 0.96 nm, respectively, and these diameters are comparable to the mean diameters of the 5%Ac-SWCNT. [11] The temperature was set to 300 K, and interatomic potentials provided with the LAMMPS package were used to describe the system. [22] The C-C interaction was described using the adaptive intermolecular reactive empirical bond order (AIREBO) potential, and the C-N and N-N interactions were described using a Lennard-Jones potential with the coefficients used by Levitt et al. [23] The  $N_2$  molecules were treated as rigid dumbbells allowing for translation and rotation of the molecules, but ignoring stretching mode vibrations.

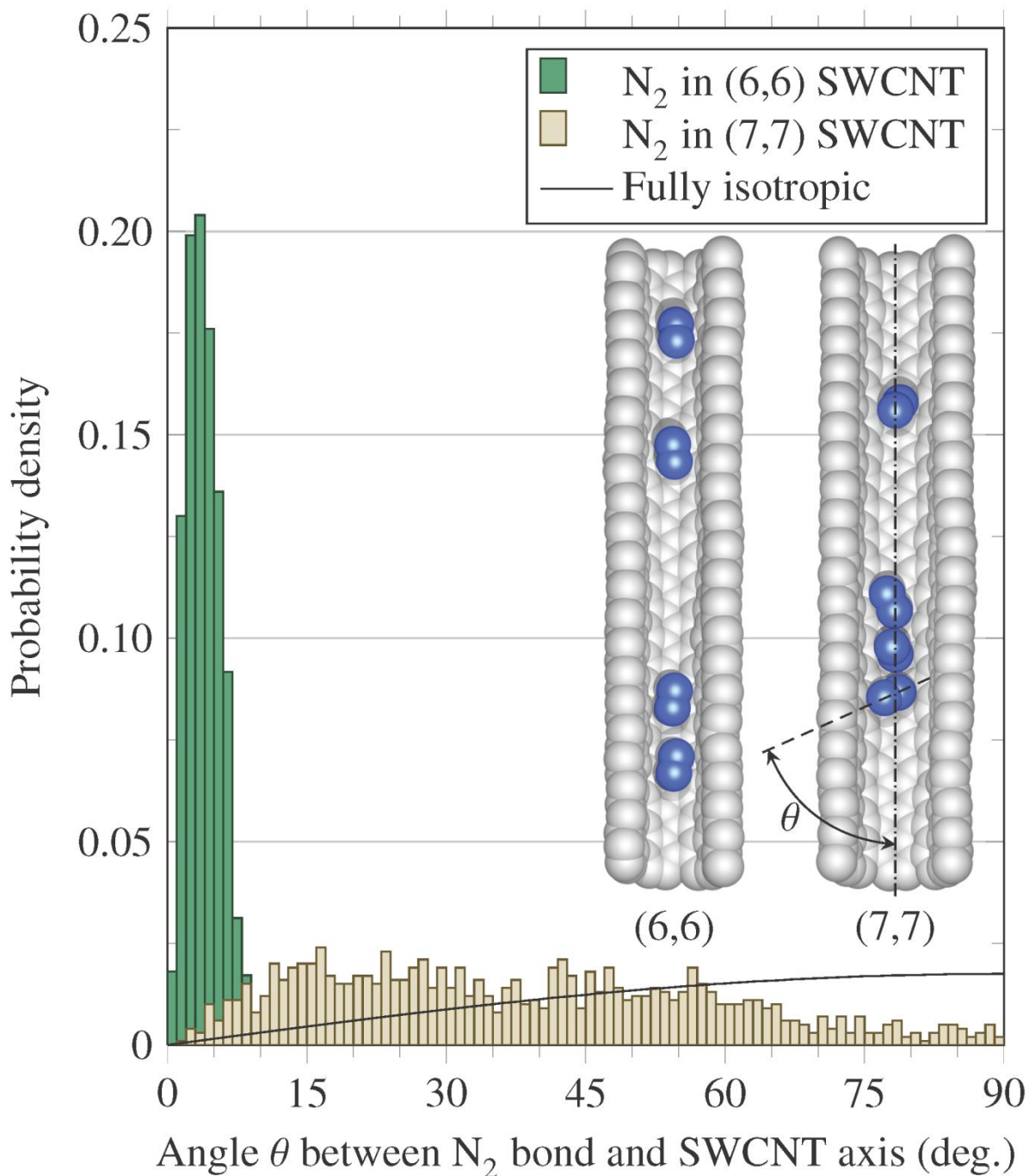


**Figure 5:** Distribution function of angle between  $N_2$  bond and the axis of the SWCNT. The insets are cuts of snapshots from the MD simulation.

Histograms showing angles between  $N_2$  bonds and the axis of their host SWCNT are presented in Figure 5. The continuous line shows the probability density distribution of a completely isotropic distribution due to growing differential solid angle  $2\pi\sin\theta d\theta$ . In the MD

simulation we find a much more pronounced co-axial alignment of  $N_2$  in the (6,6) SWCNT, yet the (7,7) SWCNT is sufficiently narrow that the  $N_2$  are still preferentially oriented along the nanotube axis. One difference is that the individual molecules can frequently flip over inside the (7,7) SWCNT, whereas we never find flipped molecules inside the (6,6) SWCNT. In neither SWCNT can one  $N_2$  molecule pass another, they always keep their original sequence.

The use of interatomic potentials in the MD fully corroborates that sub-nm thin SWCNT are large enough to hold  $N_2$  and yet tight enough to template co-axial alignment. Beyond the interatomic pair-interactions available in the LAMMPS package, the fluctuating dipoles that give rise to Van der Waals (VdW) interaction will be bound to be co-axial on diatomic  $N_2$ . The surrounding SWCNT is a one-dimensional electronic system that also offers an easy axis for fluctuating dielectric displacements. Therefore the VdW interaction is expected to favor co-axial configurations of the host SWCNT and interior  $N_2$ . Indeed aligned  $N_2$  is observed inside MWCNT and  $CN_x$  nanofibres. [5–7] The extent to which VdW interactions can also explain the observation of aligned  $N_2$  inside larger cavities will be the subject of further in-depth studies.

Our MD simulations are in agreement with the spectroscopic signatures of an aligned one dimensional arrangement of  $N_2$  molecules inside sub-nm-diameter VA-SWCNT. The narrow interior ( $d < 1$  nm) is found to confine the diatomic  $N_2$  molecules to a co-axial configuration. The encapsulated  $N_2$  form a linear system with a fixed sequence.

#### **4. Summary**

Vertically aligned forests of sub-nm thin SWCNT can be filled with  $N_2$  molecules if a mixed acetonitrile/ethanol feedstock is used during CVD synthesis. The interior space of these

SWCNT is sufficiently narrow ( $d < 1$  nm) that the contained molecules are kept in a strictly one-dimensional arrangement, as indicated by high-resolution NEXAFS measurement and corroborated by MD simulation of N<sub>2</sub> inside (6,6) and (7,7) SWCNT.

## Acknowledgements

Beamtime at SPring-8 was granted for proposal 2012A1092. Part of this work was financially supported by Grants-in-Aid for Scientific Research (19054003, 22226006, and 23760180), and the JSPS Core-to-Core Global COE Program “Global Center for Excellence for Mechanical Systems Innovation”. C.K. acknowledges the Austrian Academy of Sciences for the APART fellowship 11456. T.T. acknowledges support from the Higher Educational Strategic Scholarships for Frontier Research Network (CHE-PhD-SFR) granted by the Office of Higher Education Commission, Thailand.

## References

- [1] Smith BW, Monthieux M, Luzzi DE, Encapsulated C-60 in carbon nanotubes. *Nature* 1998;396:323–4.
- [2] Bandow S, Takizawa M, Hirahara K, Yudasaka M, Iijima S, Raman scattering study of double-wall carbon nanotubes derived from the chains of fullerenes in single-wall carbon nanotubes. *Chem Phys Lett* 2001;337:48–54.
- [3] Kitaura R, Imazu N, Kobayashi K, Shinohara H, Fabrication of metal nanowires in carbon nanotubes via versatile nano-template reaction. *Nano Lett* 2008;8:693–99.
- [4] Terrones M, Kamalakaran R, Seeger T, Ruhle M, Novel nanoscale gas containers: encapsulation of N<sub>2</sub> in CN<sub>x</sub> nanotubes. *Chem Comm* 2000:2335–36.
- [5] Okotrub AV, Bulusheva LG, Kudashov AG, Belavin VV, Vyalikh DV, Molodtsov SL, Orientation ordering of N<sub>2</sub> molecules in vertically aligned CN (x) nanotubes. *Appl Phys A* 2009;94:437–43.

- [6] Okotrub AV, Kanygin MA, Bulusheva LG, Vyalikh DV, X-ray absorption spectra of N<sub>2</sub> molecules embedded into CN<sub>x</sub> nanotubes as a marker of orientation ordering of array. Fuller Nanotu Carb Nanostr 2010;18:551–7.
- [7] Zhou JG, Wang JA, Liu H, Banis MN, Sun XL, Sham TK, Imaging nitrogen in individual Carbon Nanotubes. J. Phys. Chem. Lett. 2010;1:1709–13.
- [8] Murakami Y, Miyauchi Y, Chiashi S, Maruyama S, Direct synthesis of high-quality single-walled carbon nanotubes on silicon and quartz substrates. Chem Phys Lett 2003;377:49–54.
- [9] Murakami Y, Chiashi S, Miyauchi Y, Hu MH, Ogura M, Okubo T, et al. Growth of vertically aligned single-walled carbon nanotube films on quartz substrates and their optical anisotropy. Chem Phys Lett 2004;385:298–303.
- [10] Oshima H, Suzuki Y, Shimazu T, Maruyama S, Novel and simple synthesis method for submillimeter long vertically aligned single-walled carbon nanotubes by no-flow alcohol catalytic chemical vapor deposition. Jpn J Appl Phys 2008;47:1982–84.
- [11] Thurakitseree T, Kramberger C, Zhao P, Aikawa S, Harish S, Chiashi S, et al. Diameter-controlled and nitrogen-doped vertically aligned single-walled carbon nanotubes. Carbon 2012;50:2635–40.
- [12] Ohashi H, Ishiguro E, Tamenori Y, Okumura H, Hiraya A, Yoshida H, et al, Monochromator for a soft x-ray photochemistry beamline BL27SU of SPring-8. Nuc Instr Metho In Phys Resea A 2001;467:533–36.
- [13] Ohashi H, Ishiguro E, Tamenori Y, Kishimoto H, Tanaka M, Irie A, et al. Outline of soft x-ray photochemistry beamline BL27SU of SPring-8. Nuc Instr Metho In Phys Resea A 2001;467:529–32.
- [14] Choi HC, Bae SY, Jang W-S, Park J, Song HJ, Shin H-J, et al. Release of N<sub>2</sub> from the carbon nanotubes via high-temperature annealing. J Phys Chem B 2005;109:1683-88.

- [15] Kramberger C, Rauf H, Shiozawa H, Knupfer M, Büchner B, Pichler T, et al. Unraveling van Hove singularities in x-ray absorption response of single-wall carbon nanotubes. *Phys Rev B* 2007;75:2354371-4.
- [16] Powell CJ, Jablonski A, Evaluation of calculated and measured electron inelastic mean free paths near solid surfaces. *J Phys Chem Ref Data* 1999;28:19–62.
- [17] Abbas G, Papakonstantinou P, Iyer GRS, Kirkman IW, Chen LC, Substitutional nitrogen incorporation through rf glow discharge treatment and subsequent oxygen uptake on vertically aligned carbon nanotubes. *Phys Rev B* 2007;75: 1954291-9.
- [18] Chen CT, Ma Y, Sette F, *K*-shell photoabsorption of the N<sub>2</sub> molecule. *Phys Rev A* 1989;40:6737–40.
- [19] Esaka F, Shimada H, Imamura M, Matsubayashi N, Kikuchi T, Furuya K, Highresolution XAS spectrum of interstitial nitrogen molecules in the surface oxide matrix of TiAlN film. *J Elec Spectr Relat Phenom* 1998;88:817–20.
- [20] Petravac M, Gao Q, Llewellyn D, Deenapanray PNK, MacDonald D, Crotti C, Broadening of vibrational levels in x-ray absorption spectroscopy of molecular nitrogen in compound semiconductors. *Chem Phys Lett* 2006;425:262–66.
- [21] Yang JH, Lee DH, Yum MH, Shin YS, Kim EJ, Park CY, et al. Encapsulation mechanism of N<sub>2</sub> molecules into the central hollow of carbon nitride multiwalled nanofibers. *Carbon* 2006;44:2219–23.
- [22] Plimpton S, Fast Parallel Algorithms for Short-Range Molecular Dynamics. *J Comput Phys* 1995;117:1–19.
- [23] Levitt M, Hirshberg M, Sharon R, Daggett V, Potential-energy function and parameters for simulations of the molecular-dynamics of proteins and nucleic-acids in solution. *Comput Phys Comm.* 1995;91:215–31.

## Captions

**Figure 1:** Side view SEM images of vertically aligned Et-SWCNT synthesized from pure ethanol (left panel) and 5%Ac-SWCNT synthesized from mixed feedstock containing 5 vol.% acetonitrile (right panel).

**Figure 2:** XPS spectra of C1s (left) and N1s (right) core electrons demonstrate the narrow, asymmetric Doniach-Šunjić resonance of the pure  $sp^2$  carbon network as well as molecular  $N_2$  and incorporated nitrogen (both pyridinic and substitutional).

**Figure 3:** NEXAFS C1s spectra for different angles between the SWCNT alignment direction and the Poynting vector of the linearly polarized incident X-ray beam. Spectra are scaled to the maximum in the  $\sigma^*$  resonance.

**Figure 4:** NEXAFS spectra of the N1s in VA-SWCNT grown from 5 vol.% acetonitrile/ethanol mixed feedstock. The left stack is for different angles between the incident X-ray beam and the SWCNT alignment axis. The thinner line in the topmost panel ( $75^\circ$ ) is the N1s-silent reference from SWCNT synthesized from pure ethanol feedstock. The right panel shows a high resolution scan of the vibrational fine structure in the  $N1s \rightarrow \pi^*$  resonance and its lineshape analysis.

**Figure 5:** Distribution function of angle between  $N_2$  bond and the axis of the SWCNT. The insets are cuts of snapshots from the MD simulation.